

# Topological phase interference effects in resonant quantum tunneling of the Néel vector between nonequivalent magnetic wells in mesoscopic single-domain antiferromagnets

Rong Lü<sup>1,a</sup>, Hui Hu<sup>2</sup>, Jia-Lin Zhu<sup>2</sup>, Xiao-Bing Wang<sup>3</sup>, Lee Chang<sup>3</sup>, and Bing-Lin Gu<sup>3</sup>

<sup>1</sup> Center for Advanced Study, Tsinghua University, Beijing 100084, P.R. China

<sup>2</sup> Department of Physics, Tsinghua University, Beijing 100084, P.R. China

<sup>3</sup> Center for Advanced Study, Tsinghua University, Beijing 100084, P.R. China

Received 4 June 1999

**Abstract.** Resonant quantum tunneling of the Néel vector between nonequivalent magnetic wells is investigated theoretically for a nanometer-scale single-domain antiferromagnet with biaxial crystal symmetry in the presence of an external magnetic field applied along the easy anisotropy axis, based on the two-sublattice model. Both the Wentzel-Kramers-Brillouin exponent and the preexponential factors are evaluated in the instanton contribution to the tunneling rate for finite and zero magnetic fields by applying the instanton technique in the spin-coherent-state path-integral representation, respectively. The quantum interference or spin-parity effects induced by the topological phase term in the Euclidean action are discussed in the rate of quantum tunneling of the Néel vector. In the absence of an external applied magnetic field, the effect of destructive phase interference or topological quenching on resonant quantum tunneling of the Néel vector is evident for the half-integer excess spin antiferromagnetic nanoparticle. In the weak field limit, the tunneling rates are found to oscillate with the external applied magnetic field for both integer and half-integer excess spins. We discuss the experimental condition on the applied magnetic field which may allow one to observe the topological quenching effect for nanometer-scale single-domain antiferromagnets with half-integer excess spins. Tunneling behavior in resonant quantum tunneling of the magnetization vector between nonequivalent magnetic wells is also studied for a nanometer-scale single-domain ferromagnet by applying the similar technique, but in the large noncompensation limit.

**PACS.** 03.65.Bz Foundations, theory of measurement, miscellaneous theories (including Aharonov-Bohm effect, Bell inequalities, Berry's phase) – 75.45.+j Macroscopic quantum phenomena in magnetic systems – 75.50.Ee Antiferromagnetics

## 1 Introduction

Macroscopic quantum phenomena (MQP) have been given extensive investigation from both experimental and theoretical aspects for more than one decade since the pioneering work of Calderia and Leggett [1,2]. Calderia and Leggett predicted that quantum tunneling in the macroscopic domain was theoretically possible, provided that the dissipation resulting from the interaction of the macroscopic system with the environment is small enough at sufficiently low temperatures [1,2]. They presented a formalism which could incorporate the dissipation by applying the imaginary-time path integral and the standard instanton technique, and they concluded that the rate of quantum tunneling was reduced by dissipation in general [1–4]. The Calderia-Leggett approach has been considered extensively in systems of Josephson junc-

tions [5–7] and superconducting quantum interference devices (SQUIDS) [8], where the macroscopic degree of the freedom is the difference between the phases of the condensates of Cooper pairs in the superconductors on either side of the tunneling barrier.

In recent years, owing mainly to the rapid advances both in new technologies of miniaturization and in highly sensitive SQUID magnetometry, there have been considerable theoretical and experimental studies carried out on the nanometer-scale magnetic systems which exhibit macroscopic quantum coherence (MQC) and macroscopic quantum tunneling (MQT). For a single-domain ferromagnetic (FM) nanoparticle at sufficiently low temperatures, all the spins are locked together by the strong exchange interaction, and therefore only the orientation of the total magnetization vector can change but not its absolute value (Stoner-Wohlfart model). The energy of a single-domain FM nanoparticle depends on the orientation of the total magnetization vector. In such a single-domain

<sup>a</sup> e-mail: rlu@castu.phys.tsinghua.edu.cn

FM nanoparticle, the magnetocrystalline anisotropy and the external applied magnetic field can create easy directions for the total magnetization vector which correspond to local minima of magnetic energy. In the phenomenon of MQC, the magnetization vector resonates coherently between the energetically degenerate easy directions in the absence of an external applied magnetic field, thus, MQC occurs when all the spins coherently oscillate back and forth between two equivalent wells separated by a classically impenetrable barrier. However, the ground-state tunneling level splittings of single-domain FM nanoparticles are too small to be observed without controlling the height and the width of the barrier formed by the magnetocrystalline anisotropy energy at zero magnetic field. It has been believed that an applied magnetic field is a good external parameter to make the phenomena of MQT and MQC observable. By applying an external magnetic field at a proper direction to the easy anisotropy axis, one of the two energetically equivalent orientations becomes metastable and the magnetization vector can escape from the metastable state through the classically impenetrable barrier to a stable one (*i.e.*, MQT). Applications of the phenomena of MQT and MQC have been discussed in the reliability of small magnetic units in memory devices, and in quantum computers [32,33]. The phenomena of MQT and MQC will be crucial for future magnetic devices working on a nanometer-scale. Notable examples of the magnetic MQP are quantum tunneling of the magnetization vector in single-domain FM nanoparticles [9–11], quantum nucleation of the FM bubbles [12] and quantum depinning of FM domain walls from defects in bulk ferromagnets at sufficiently low temperatures [13–15]. A number of experiments [16–19] involving resonance measurements, magnetic relaxation and hysteresis loop studies have shown either temperature-independent relaxation phenomena or a well-defined resonance depending exponentially on the number of total spins of magnets, which strongly support the idea of quantum magnetic tunneling.

It has been pointed out that the single-domain antiferromagnetic (AFM) nanoparticle, which has a nonzero magnetization moment due to the small noncompensation of two sublattices, is a better candidate for observing the phenomena of MQT and MQC, compared with the single-domain FM nanoparticle of a similar size. To see this, note that for such quantum tunneling problems, the difference between the single-domain FM and AFM nanoparticles originates from the configurations of spins in the classical states. The spins remain exactly parallel in the single-domain ferromagnet. But in the single-domain antiferromagnet, the spins in two sublattices are tipped with respect to one another. The effect of the canting of the AFM spins in the barrier state is that the torques on them are much stronger than in the FM case. Thus, the resonance frequency in one of the wells separated by magnetocrystalline anisotropies or external applied magnetic fields is much larger in the single-domain AFM particle than in the FM case (we give a formula for these in the following calculation). As the rate of quantum tunneling  $\Gamma \propto \exp(-U/\hbar\omega_p)$ , where  $U$  is the magnetic barrier between two wells and

$\omega_p$  is the small-angle precession or resonance frequency in the well, the rate of quantum tunneling in single-domain AFM nanoparticles is much larger than that in single-domain FM nanoparticles of a comparable size. This makes the nanometer-scale single-domain antiferromagnets more interesting for experimental studies. By applying a fully integrated thin-film dc-SQUID micro-susceptometer, Awschalom *et al.* [19] have made low-temperature measurements of the frequency-dependent magnetic noise  $S(\omega)$  and magnetic susceptibility  $\chi(\omega)$  on nanometer-scale horse-spleen ferritin particle, a naturally occurring, antiferromagnetic, iron storage protein. These proteins contain a 7.5-nm-dim magnetic core with about 4500  $\text{Fe}^{3+}$  spin 5/2 ions below 200 mK. Although the ferritin particles are basically antiferromagnetic, they have a small uncompensated moment which allows one to probe their dynamics by measuring  $S(\omega)$  and  $\chi(\omega)$ . Awschalom *et al.* have observed a well-defined resonance below roughly 200 mK in both  $S(\omega)$  and the imaginary part,  $\chi''(\omega)$ , of  $\chi(\omega)$ , which can be interpreted as a manifestation of resonant quantum tunneling of the Néel vector between energetically degenerate easy directions in the absence of an external magnetic field. And the frequency of this resonance was found to be 2000 times higher than that of nanometer-scale ferromagnets [16]. The phenomena of MQT and MQC of the Néel vector were investigated theoretically for the single-domain AFM nanoparticles based on the two-sublattice model [20,21,23,24] and the anisotropic  $\sigma$  model [22] independently. And the phenomenon of MQT is also very important in the problems of quantum nucleation of the AFM bubbles [22,23] and quantum depinning of the domain walls from defects in bulk antiferromagnets at sufficiently low temperatures [20].

One of the most striking effects in the magnetic MQP is that for some spin systems with high symmetries, the behaviors of quantum tunneling of the magnetization vector seem sensitive to the parity of total spin of the single-domain magnet. It has been theoretically demonstrated that the ground-state tunneling level splitting is completely suppressed to zero for the half-integer total spin FM nanoparticles with biaxial crystal symmetry in the absence of an external applied magnetic field, resulting from the destructive interference of the Berry phase or the Wess-Zumino, Chern-Simons term in the magnetic action between the symmetry-related tunneling paths connecting two classically degenerate minima [25,26]. Such a destructive phase interference effect for the single-domain FM nanoparticles with half-integer total spins is known as the topological quenching [27]. But for integer total spin FM nanoparticles, the quantum phase interference between topologically different tunneling paths is constructive, and therefore the ground-state tunneling level splitting is nonzero. A similar topological phase interference or spin-parity effect has been found theoretically in the single-domain AFM nanoparticle with biaxial crystal symmetry in the absence of an external applied magnetic field, in which only an integer excess spin AFM particle can tunnel coherently between energetically degenerate easy directions, but not a half-integer excess

spin one [21,22]. Similar effects have been observed in one-dimensional antiferromagnetic Heisenberg spin chains where the ground state has a finite gap (Haldane gap [38]) in spin excitation for integer spin, while such gaps are suppressed to zero for half-integer spin, resulting from the destructive interference of topological Berry phases [39]. However, these topological phase interference effects are intrinsically absent in the Josephson-junction-based superconducting systems [4–8], which makes quantum tunneling phenomena in nanometer-scale single-domain magnets more important for understanding the foundations of quantum mechanics. Theoretical studies have shown that the destructive phase interference or topological quenching effect in magnetization tunneling could also be unrelated to the Kramers' degeneracy in the FM [27] and AFM [28] spin systems, where an external magnetic field is applied at a right angle to break the time-reversal invariance of the systems. Recently, the topological phase interference effect in resonant quantum tunneling of the magnetization vector between nonequivalent wells formed by the external applied magnetic field has been studied extensively in the single-domain FM nanoparticles [29,30]. Motivated by the theoretical works on single-domain FM nanoparticles [29,30], in the present work we will study the spin-parity or topological phase interference effects in the resonant quantum tunneling of the Néel vector between nonequivalent wells in the single-domain AFM nanoparticles with biaxial crystal symmetry in the presence of an external magnetic field applied along the easy anisotropy axis of the system, opposite to the direction of the Néel vector. Besides its importance in the phenomena of MQT and MQC in magnets from the fundamental point of view [31], the quantum interference effects induced by the topological phase coherence between symmetry-related tunneling paths are found to be potentially important in the designing of quantum computers in the future [32,33]. One recent experimental method based on the Landau-Zener model was developed by Wernsdorfer and Sessoli [40] to measure very small tunneling splittings on the order of  $10^{-8}$  K in an octanuclear iron(III) oxo-hydroxo cluster of formula  $[\text{Fe}_8\text{O}_2(\text{OH})_{12}(\text{tacn})_6]^{8+}$ ,  $\text{Fe}_8$ , where tacn is the organic ligand triazacyclononane. At sufficiently low temperatures, the molecular  $\text{Fe}_8$  cluster behaves like a nanomagnet with a spin ground state of  $S = 10$ , which arises from competing antiferromagnetic interactions between the eight  $S = 5/2$  iron spins. Wernsdorfer and Sessoli have observed a very clear oscillation of the tunneling splitting as a function of the magnetic field applied along the hard anisotropy axis, which is direct evidence of the role of the topological spin phase (Berry phase) in the spin dynamics of these molecules.

The purpose of the present work is to investigate theoretically the topological phase interference or spin-parity effects in resonant quantum tunneling of the Néel vector between nonequivalent wells separated by the magnetocrystalline anisotropy and the external applied magnetic field in a single-domain AFM nanoparticle with biaxial crystal symmetry at sufficiently low temperatures, based on the two-sublattice model. The phenomenon of

MQT in the single-domain AFM nanoparticle corresponds to the escape of the Néel vector through the classically impenetrable barrier from a metastable state (*i.e.*, the local minimum of the magnetic energy) to a stable one by quantum tunneling. The simplest way to obtain the metastable state is to apply an external magnetic field at right angles to the easy anisotropy axis of the system. In the present work, the external magnetic field is assumed to be applied along the easy anisotropy axis of the system, opposite to the direction of the Néel vector, which creates the nonequivalent wells in the basal plane. Both the Wentzel-Kramers-Brillouin (WKB) exponent and the preexponential factors are evaluated in the instanton contribution to the rate of quantum tunneling of the Néel vector for the entire region of the external magnetic field ( $0 \leq H < H_c$ ) by applying of the standard instanton technique in the spin-coherent-state path-integral representation [11,24,35–37], where  $H_c$  is the coercive field. The oscillation of the WKB tunneling rate with the external applied magnetic field is clearly shown, and the experimental condition of the applied magnetic field is suggested for observing the destructive phase interference or topological quenching effect in nanometer-scale single-domain antiferromagnets with half-integer excess spins. It is noted that in reference [28], the tunneling behaviors have been studied in resonant quantum tunneling of the Néel vector between energetically equivalent wells separated by the external magnetic field along the hard anisotropy axis of the system (compared with the easy anisotropy axis in this paper). The results show that the tunneling properties of the Néel vector between equivalent wells [28] are significantly different from those of the Néel vector between nonequivalent wells considered in the present work. Note that the calculation of tunneling rate for the nanometer-scale single-domain antiferromagnet is performed in the small noncompensation limit, at which the excess spin of the single-domain AFM nanoparticle owing to the noncompensation of two sublattices is much smaller than the sublattice spin. And it is easy to obtain the topological phase interference or spin-parity effects in resonant quantum tunneling of the magnetization vector between nonequivalent wells for nanometer-scale single-domain ferromagnets with biaxial crystal symmetry in the presence of an external magnetic field applied along the easy anisotropy axis by making use of the similar technique, but in the large noncompensation limit.

The system of interest is a single-domain AFM nanoparticle of about 5 nm in radius at a temperature well below its anisotropy gap. Let us assume a simple two-sublattice AFM particle, and denote the sublattices by 1 and 2 respectively. According to the two-sublattice model [20], there is a strong exchange energy  $\mathbf{m}_1 \cdot \mathbf{m}_2 / \chi_\perp$  between two sublattices, where  $\mathbf{m}_1$  and  $\mathbf{m}_2$  are the magnetization vectors of two sublattices with large, fixed and unequal magnitudes, and  $\chi_\perp$  is the transverse susceptibility. Under the assumption that the exchange energy between two sublattices is much larger than the magnetocrystalline anisotropy energy and the Zeeman energy when an external magnetic field is applied, the Euclidean action for the small noncompensated AFM nanoparticle (neglecting

the dissipation with the environment) is given by [20]

$$S_E[\theta(\mathbf{x}, \tau), \phi(\mathbf{x}, \tau)] = \frac{1}{\hbar} \int d\tau \int d^3x \left\{ i \frac{m_1 + m_2}{\gamma} \left( \frac{\partial \phi}{\partial \tau} \right) + \frac{\chi_{\perp}}{2\gamma^2} \left[ \left( \frac{\partial \theta}{\partial \tau} \right)^2 + \left( \frac{\partial \phi}{\partial \tau} \right)^2 \sin^2 \theta \right] + \frac{1}{2} \alpha [(\nabla \theta)^2 + (\nabla \phi)^2 \sin^2 \theta] + E(\theta, \phi) \right\}, \quad (1)$$

where  $\gamma$  is the gyromagnetic ratio,  $\tau = it$  is the imaginary time, and  $\alpha$  is the exchange constant. We assume that  $m_1 > m_2$  and  $m = m_1 - m_2 \ll m_1$ . The  $E(\theta, \phi)$  term in the above equation includes the magnetocrystalline anisotropy and the Zeeman energies. The polar coordinate  $\theta$  and the azimuthal coordinate  $\phi$ , which are the angular components of  $\mathbf{m}_1$  in the spherical coordinate system, determine the direction of the Néel vector in single-domain AFM nanoparticle.

As pointed out in reference [20], for a nanometer-scale single-domain antiferromagnet, the Néel vector may depend on the imaginary time but not on coordinates because spatial derivatives in equation (1) are suppressed by the strong exchange interaction between two sublattices ( $\mathbf{m}_1 \cdot \mathbf{m}_2 / \chi_{\perp}$ ). The spatial derivatives in equation (1) are important in the problems of quantum tunneling in nonuniform magnetic structure, such as quantum nucleation in a thin film or quantum depinning of domain wall in bulk magnets at sufficiently low temperatures. So all the calculations performed in the present work are for the case of the homogeneous Néel vector. Therefore, equation (1) reduces to

$$S_E(\theta, \phi) = \frac{V}{\hbar} \int d\tau \left\{ i \frac{m_1 + m_2}{\gamma} \left( \frac{d\phi}{d\tau} \right) + \frac{\chi_{\perp}}{2\gamma^2} \left[ \left( \frac{d\theta}{d\tau} \right)^2 + \left( \frac{d\phi}{d\tau} \right)^2 \sin^2 \theta \right] + E(\theta, \phi) \right\}, \quad (2)$$

where  $V$  is the volume of the single-domain AFM nanoparticle.

In the spin-coherent-state representation, the  $\mathbf{m}_1$  state can be characterized by the angles  $\theta$  and  $\phi$  as

$$|\theta, \phi\rangle = \left( \cos \frac{\theta}{2} \right)^{2S} \exp \left( \tan \frac{\theta}{2} e^{i\phi} \hat{S}^- \right) |S\rangle. \quad (3)$$

The spin coherent state is defined as the maximum eigenstate of  $\hat{S}_z$ , rotated into the direction of the unit vector  $\mathbf{n} = (\sin \theta \cos \phi, \sin \theta \sin \phi, \cos \theta)$ . Compared with the FM case in reference [29], now  $S = m_1 V / \hbar \gamma$  is the total spin in one sublattice for the single-domain AFM nanoparticle.  $\hat{S}^- = \hat{S}_x - i\hat{S}_y$ , and  $|S\rangle$  is the eigenstate of  $\hat{S}_z$  corresponding to the maximal eigenvalue  $S_z = S$ .

The system is supposed to have an easy anisotropy axis along  $\mathbf{x}$  and an easy plane in the  $x - y$  plane. In the presence of an external magnetic field  $\mathbf{H}$  applied along the

easy  $\mathbf{x}$  axis, opposite to the direction of the Néel vector, the  $E(\theta, \phi)$  term in equation (2) can be expressed as

$$E(\theta, \phi) = K_{\perp} \cos^2 \theta + K_{\parallel} \sin^2 \theta \sin^2 \phi - mH(1 - \sin \theta \cos \phi), \quad (4)$$

where  $K_{\perp}$  and  $K_{\parallel}$  are the transverse and longitudinal anisotropy coefficients respectively. Like the problem considered in reference [20], in the present work we also assume that the transverse anisotropy coefficient is much larger than the longitudinal one, which agrees with the experimental situation for highly anisotropic materials (such as rare-earth materials).

When  $H \neq 0$ , there is a metastable state at  $\theta = \pi/2$ ,  $\phi = 0$  (*i.e.*, the Néel vector antiparallel to the external applied magnetic field) and a stable state at  $\theta = \pi/2$ ,  $\phi = \pi$  (*i.e.*, the Néel vector parallel to the external applied magnetic field). The energy maximum of the system corresponds to  $\theta = \pi/2$  and  $\cos \phi_1 = H/H_c$ , where  $H_c = 2K_{\parallel}/m$ .  $H_c$  is the coercive field at which the initial state becomes classically unstable. It is noted that there also exists a spin-flop field for single-domain AFM nanoparticles at finite magnetic field,  $H_{s.f.}$ , which can rotate the magnetization moments of sublattices away from the anisotropy axis. The spin-flop field is defined as  $H_{s.f.} = \sqrt{2H_{\parallel}H_{ex}}$ , with  $H_{\parallel} = 2K_{\parallel}/m_1$  being the longitudinal anisotropy field, and  $H_{ex} = J/m_1$  being the exchange field between sublattices, where  $J$  is the exchange energy density between two sublattices. Therefore, the actual applied field must be the smallest of these two fields, where the two-sublattice configuration is still valid for single-domain AFM nanoparticles at finite magnetic field.

To decay out of the metastable state, the Néel vector must rotate by the angle  $\pm \phi_2$ , which satisfies

$$\sin^2 \left( \frac{\phi_2}{2} \right) = \epsilon, \quad (5)$$

where  $\epsilon = 1 - H/H_c$ . Now the problem is one of resonant MQT, *i.e.*, the escaping of the Néel vector through the magnetic barrier by quantum tunneling from the initial  $\Psi_0$  level to the excited  $\Psi_r$  level which is in resonance with  $\Psi_0$  at finite magnetic field.

The amplitude of such resonant quantum transition is given by the imaginary-time propagator

$$A = \langle \Psi_0 | e^{-HT} | \Psi_r \rangle. \quad (6)$$

In the semiclassical approximation, the  $\Psi_0$  state is very close to  $|\pi/2, 0\rangle$ . Then the above equation reduces to

$$A \approx \langle \pi/2, 0 | e^{-HT} | \pi/2, -\phi_2 \rangle \langle \pi/2, -\phi_2 | \Psi_r \rangle + \langle \pi/2, 0 | e^{-HT} | \pi/2, \phi_2 \rangle \langle \pi/2, \phi_2 | \Psi_r \rangle. \quad (7)$$

In the limit that  $T \rightarrow \infty$ , the propagator

$$\langle \pi/2, 0 | e^{-HT} | \pi/2, \phi_2 \rangle \rightarrow \exp [i(2S - s)\phi_2] \exp(-E_0 T),$$

where  $E_0$  is the energy of the metastable state  $\Psi_0$ .  $S = m_1 V / \hbar \gamma$  is the total spin in one sublattice,

$s = mV/\hbar\gamma$  is the excess spin of single-domain AFM nanoparticle owing to the small noncompensation of two sublattices ( $s \ll S$ ). Since the state  $\Psi_0$  is unstable,  $E_0$  will have an imaginary part, which is related to the decay rate  $\Gamma$  by the usual formula:  $\Gamma = -2\Im E_0$  [11, 35–37]. Therefore, the propagator  $\langle \pi/2, 0 | e^{-HT} | \pi/2, \phi_2 \rangle$  becomes  $\exp[i(2S - s)\phi_2] \exp(-\hbar\omega_p T/2) \exp(i\Gamma T/2)$ , where  $\omega_p$  is the oscillation frequency in the well.

The propagators  $\langle \pi/2, 0 | e^{-HT} | \pi/2, \pm\phi_2 \rangle$  in equation (7) are equivalent to the following imaginary-time path integral in the spin-coherent-state representation,

$$\int D\{\theta\} D\{\phi\} \exp[-S_E(\theta, \phi)], \quad (8)$$

over the classical trajectories connecting the initial state  $|\pi/2, 0\rangle$  and the final states  $|\pi/2, \pm\phi_2\rangle$ , where the Euclidean action  $S_E(\theta, \phi)$  has been defined in equation (2). Now the calculation of the WKB escaping rate for this resonant quantum tunneling problem consists of two major steps. The first step is to evaluate the propagators  $\langle \pi/2, 0 | e^{-HT} | \pi/2, \pm\phi_2 \rangle$ . This can be performed with the help of the standard instanton technique in the spin-coherent-state path-integral representation [11, 24, 35–37]. The second step is to calculate the overlap factors  $\langle \pi/2, \pm\phi_2 | \Psi_T \rangle$ . In reference [24], Lü *et al.* have investigated the general formulas for calculating both the WKB exponent and the preexponential factors in the tunneling rate  $\Gamma$  (in MQT problems) or the tunneling level splitting  $\Delta$  (in MQC problems) for nanometer-scale single-domain antiferromagnets based on the two-sublattice model and the instanton technique in the spin-coherent-state path-integral representation, without assuming a specific form of the magnetocrystalline anisotropy and the external magnetic field. In Appendix A of this paper, we discuss briefly the basic idea of this calculation.

To execute the first step, we must find the classical path  $(\bar{\theta}, \bar{\phi})$  which minimizes the Euclidean action  $S_E(\theta, \phi)$  of equation (2). It is noted that the first term in the Euclidean action of equation (2) is a total imaginary-time derivative, which has no effect on the classical equations of motion for the Néel vector in single-domain AFM nanoparticles, but yields a boundary contribution to the Euclidean action. However, we will show in the following that this term, known as the topological phase term, is of crucial importance to the quantum interference effects in nanometer-scale single-domain antiferromagnets and makes the tunneling behaviors of integer and half-integer excess spins strikingly different. We ignore this topological phase interference or spin-parity effect for the moment, but focus on the evaluation of the instanton's contribution to the WKB escaping rate for resonant quantum tunneling of the Néel vector between nonequivalent magnetic wells in single-domain AFM nanoparticles with biaxial crystal symmetry in the presence of an external magnetic field applied along the easy anisotropy axis. Then we reinstate the phase factors generated by the topological term in the Euclidean action in the final expression for the quantum escaping rate.

The classical path  $(\bar{\theta}, \bar{\phi})$  obeys the following equations of motion for the Néel vector in single-domain AFM nanoparticles ( $\delta S_E = 0$ ),

$$\begin{aligned} \frac{\chi_\perp}{\gamma^2} \frac{d^2 \bar{\theta}}{d\tau^2} &= \frac{\chi_\perp}{\gamma^2} \left( \frac{d\bar{\phi}}{d\tau} \right)^2 \sin \bar{\theta} \cos \bar{\theta} + \frac{\partial E}{\partial \bar{\theta}}, \\ \frac{\chi_\perp}{\gamma^2} \frac{d}{d\tau} \left[ \left( \frac{d\bar{\phi}}{d\tau} \right) \sin^2 \bar{\theta} \right] &= \frac{\partial E}{\partial \bar{\phi}}. \end{aligned} \quad (9)$$

In the case of very strong transverse anisotropy, the Néel vector is forced to lie in the  $x$ - $y$  plane. Substituting equation (4) into the classical equations of motion for the Néel vector in single-domain AFM nanoparticles, we obtain the instanton solution for  $0 < \epsilon < 1$ ,

$$\begin{aligned} \bar{\theta} &= \frac{\pi}{2}, \\ \sin^2 \left( \frac{\bar{\phi}}{2} \right) &= \frac{1 - \tanh^2(\omega_0 \sqrt{\epsilon} \tau)}{\lambda - \tanh^2(\omega_0 \sqrt{\epsilon} \tau)}, \end{aligned} \quad (10)$$

where  $\lambda = 1/\epsilon$  and  $\omega_0 = \gamma\sqrt{2K_{\parallel}/\chi_{\perp}}$ . The corresponding classical action, *i.e.*, the WKB exponent in the rate of quantum tunneling at finite magnetic field, can be evaluated by integrating the Euclidean action (2) with the above classical trajectories, and the result is found to be

$$S_{\text{cl}} = 2^{3/2} \frac{V}{\hbar\gamma} \sqrt{\chi_{\perp} K_{\parallel}} \left[ \sqrt{\epsilon} - \frac{1}{2}(1 - \epsilon) \ln \left( \frac{1 + \sqrt{\epsilon}}{1 - \sqrt{\epsilon}} \right) \right]. \quad (11)$$

The preexponential factors in the instanton's contribution to the WKB tunneling rate are related to the quantum fluctuations about the classical path, which can be evaluated by expanding the Euclidean action of equation (2) to second order in small fluctuations [24] (for the detailed calculation see Appendix A).

After evaluating the preexponential factors due to the small fluctuations about the classical path, we obtain the instanton's contribution to the WKB rate for resonant quantum tunneling of the Néel vector between nonequivalent wells at finite magnetic field as the following equation [24],

$$\begin{aligned} \Gamma_{\text{AFM}} &= \frac{2^{9/4}}{\pi^{1/2}} \frac{V}{\hbar} K_{\perp} \left( \frac{K_{\parallel} J}{K_{\perp}^2} \right)^{3/4} \frac{\epsilon^{5/4}}{\sqrt{1 - \epsilon}} \\ &\times \left[ 1 - \left( \frac{K_{\parallel}}{K_{\perp}} \right) \left( \frac{H}{H_c} \right) \right]^{-1/2} \left( \frac{1 + \sqrt{\epsilon}}{1 - \sqrt{\epsilon}} \right)^3 \frac{\left( \frac{K_{\parallel}}{K_{\perp}} \right) \left( \frac{H}{H_c} \right)}{1 - \left( \frac{K_{\parallel}}{K_{\perp}} \right) \left( \frac{H}{H_c} \right)} \sqrt{\epsilon} \\ &\times \exp \left[ -4 \frac{\left( \frac{K_{\parallel}}{K_{\perp}} \right)}{1 - \left( \frac{K_{\parallel}}{K_{\perp}} \right) \left( \frac{H}{H_c} \right)} \epsilon \right] S^{-1/2} e^{-S_{\text{cl}}}, \end{aligned} \quad (12)$$

where  $S = m_1 V/\hbar\gamma$  is the total spin in one sublattice, and  $J (= \hbar^2 \gamma^2 S^2 / \chi_{\perp} V^2)$  is the exchange energy density between two sublattices.

Suppose the excess spin of the single-domain AFM nanoparticle is solely due to the small noncompensation

of two sublattices at the particle surface. It has been argued [20] that for a single-domain AFM nanoparticle with  $N$  spins,  $N^{2/3}$  spins are at the surface, thus the number of excess spins due to statistical fluctuations of the particle shape is about  $(N^{2/3})^{1/2} = N^{1/3}$ . For a nanometer-scale single-domain antiferromagnet of about  $10^3$  spins, the number of excess spins would be 10, which is a small fraction of the  $N \sim 10^3$  spins in the particle.

In terms of the exchange energy density  $J$  between two sublattices and the sublattice spin  $S$ , the classical action or the WKB exponent of equation (11) for the small noncompensated AFM nanoparticle can be rewritten as

$$S_{\text{cl}} = 2^{3/2} \sqrt{\frac{K_{\parallel}}{J}} S \left[ \sqrt{\epsilon} - \frac{1}{2}(1 - \epsilon) \ln \left( \frac{1 + \sqrt{\epsilon}}{1 - \sqrt{\epsilon}} \right) \right]. \quad (13)$$

Both the WKB exponent and the preexponential factors are clearly shown in equations (12, 13) for the entire region of the magnetic field ( $0 < H < H_c$ ), which may be helpful for the experimental investigation of the phenomenon of resonant quantum tunneling of the Néel vector in single-domain AFM nanoparticles in the presence of an external applied magnetic field along the easy anisotropy axis.

It is noted that equations (12, 13) are obtained for the small noncompensation case, *i.e.*,  $m \ll \sqrt{2K_{\perp}\chi_{\perp}}$ . On the other hand for the large noncompensation case, *i.e.*,  $m \gg \sqrt{2K_{\perp}\chi_{\perp}}$ , the problem reduces to one of resonant quantum tunneling of the magnetization vector in single-domain FM nanoparticles [29]. However, in reference [29], the instanton solution, the associated WKB exponent and the preexponential factors are not clearly shown in the instanton contribution to the WKB escaping rate for resonant quantum tunneling of the magnetization vector between nonequivalent wells for nanometer-scale single-domain ferromagnets with biaxial crystal symmetry at finite magnetic field. Here, by applying a technique similar to that for the single-domain AFM nanoparticle, we obtain the instanton contribution to the WKB tunneling rate for the single-domain FM nanoparticle at finite magnetic field as the following equation,

$$\begin{aligned} \Gamma_{\text{FM}} &= \frac{8}{\pi^{1/2}} \frac{V}{\hbar} K_{\perp} \left( \frac{K_{\parallel}}{K_{\perp}} \right)^{3/4} \frac{\epsilon^{5/4}}{\sqrt{1 - \epsilon}} \\ &\times \left[ 1 - \left( \frac{K_{\parallel}}{K_{\perp}} \right) \left( \frac{H}{H_c} \right) \right]^{-1/2} \\ &\times \exp \left[ -2 \left( \frac{K_{\parallel}}{K_{\perp}} \right) \epsilon \right] (S')^{-1/2} e^{-S'_{\text{cl}}}, \quad (14) \end{aligned}$$

where  $S'$  is the total spin of the single-domain FM nanoparticle. Now  $H_c = 2K_{\parallel}/M_0$  is the coercive field for the single-domain FM nanoparticle at which the initial state becomes classically unstable, where  $M_0 = \hbar\gamma S'/V$  is the magnitude of the total magnetization moment. And the associated classical action  $S'_{\text{cl}}$  for the single-domain FM nanoparticle is found to be

$$S'_{\text{cl}} = 2 \sqrt{\frac{K_{\parallel}}{K_{\perp}}} S' \left[ \sqrt{\epsilon} - \frac{1}{2}(1 - \epsilon) \ln \left( \frac{1 + \sqrt{\epsilon}}{1 - \sqrt{\epsilon}} \right) \right]. \quad (15)$$

The limiting cases for  $H \rightarrow 0$  and  $H \rightarrow H_c$  of the WKB exponent in equation (15) agree exactly with the results in reference [9]. However, we emphasize that the above formulas (14, 15) obtained for the single-domain FM nanoparticle are valid for the entire region of the external magnetic field ( $0 < H < H_c$ ) applied along the easy anisotropy axis, opposite to the direction of the magnetization vector. This provides a controllable parameter for experimental observation of the phenomenon of resonant quantum tunneling of the magnetization vector in single-domain FM nanoparticles.

Now we turn to the second step for resonant quantum tunneling of the Néel vector between nonequivalent wells in single-domain AFM nanoparticles with biaxial crystal symmetry placed in a magnetic field along the easy anisotropy axis, *i.e.*, the evaluation of the overlap factors  $\langle \pi/2, \pm\phi_2 | \Psi_r \rangle$ . The excited resonant state  $|\Psi_r\rangle$  can be expanded in terms of the eigenstates of  $\hat{S}_z$  as

$$|\Psi_r\rangle = \sum_{S_z} a_{S_z}(H) |S_z\rangle. \quad (16)$$

Due to the symmetry of the system,  $a_{S_z}$  are either all even,  $a_{S_z} = a_{-S_z}$ , or all odd,  $a_{S_z} = -a_{-S_z}$ , in  $S_z$ . With the help of equation (3),  $|\pi/2, \pm\phi_2\rangle$  can be expanded as

$$|\pi/2, \pm\phi_2\rangle = e^{\pm i\phi_2 S} \sum_{S_z} e^{\mp i\phi_2 S_z} b_{S_z} |S_z\rangle, \quad (17)$$

where

$$b_{S_z} = 2^{-S} \left[ \frac{(2S)!}{(S - S_z)!(S + S_z)!} \right]^{1/2}. \quad (18)$$

It is easy to show that  $b_{S_z}$  are all even,  $b_{S_z} = b_{-S_z}$ , in  $S_z$ . All the expansions in equations (16, 17) are performed in terms of the eigenstates of  $S_z$  for the single-domain AFM nanoparticle, compared with the FM case in reference [29].

After evaluating the overlap factors and combining all terms in equation (7), we obtain the transition amplitude that corresponds to the resonant quantum transition of the Néel vector through the magnetic barrier from  $\Psi_0$  level to an even-symmetry  $\Psi_r$  level in nanometer-scale single-domain antiferromagnets as the following equations [11, 35–37],

$$\begin{aligned} A_{\text{AFM}} &= \exp(-\hbar\omega_p T/2) \exp(i\Gamma_{\text{AFM}} T/2) \\ &\times \cos[(S - s)\phi_2] \sum_{m=0}^S C_m \cos(m\phi_2), \quad (19) \end{aligned}$$

for an integer  $S$ , and

$$\begin{aligned} A_{\text{AFM}} &= \exp(-\hbar\omega_p T/2) \exp(i\Gamma_{\text{AFM}} T/2) \\ &\times \cos[(S - s)\phi_2] \sum_{m=0}^{S-1/2} C_m \cos \left[ \left( m + \frac{1}{2} \right) \phi_2 \right], \quad (20) \end{aligned}$$

for a half-integer  $S$ , where  $\Gamma_{\text{AFM}}$  is shown in equation (12), and  $\omega_p = \omega_0 \sqrt{\epsilon} = (V/\hbar S) \sqrt{2K_{\parallel} J \epsilon}$  is the oscillation frequency in the well for nanometer-scale single-domain antiferromagnets at finite magnetic field.  $S$  is the total spin in

one sublattice and  $s$  is the excess spin of the single-domain AFM nanoparticle owing to the small noncompensation of two sublattices ( $s \ll S$ ). Here,  $C_m = ka_{S_z} b_{S_z}$ , with  $S_z = m$  for an integer  $S$  and  $S_z = m + 1/2$  for a half-integer  $S$ ;  $k = 2$  if  $S_z = 0$  and  $k = 4$  for all  $S_z \neq 0$ . The WKB tunneling rate corresponding to the resonant quantum transition of the Néel vector to an odd-symmetry  $\Psi_r$  level is found to be zero.

It is easy to show that in the large noncompensation limit, equations (19, 20) reduces to the following equations for resonant quantum tunneling of the magnetization vector between nonequivalent magnetic wells for single-domain FM nanoparticles with biaxial crystal symmetry in the presence of an external magnetic field applied along the easy anisotropy axis [11, 35–37],

$$A_{\text{FM}} = \exp(-\hbar\omega_p T/2) \exp(i\Gamma_{\text{FM}} T/2) \sum_{m=0}^{S'} C_m \cos(m\phi_2), \quad (21)$$

for an integer  $S'$ , and

$$A_{\text{FM}} = \exp(-\hbar\omega_p T/2) \exp(i\Gamma_{\text{FM}} T/2) \times \sum_{m=0}^{S'-1/2} C_m \cos\left[\left(m + \frac{1}{2}\right)\phi_2\right], \quad (22)$$

for a half-integer  $S'$ , where  $\Gamma_{\text{FM}}$  is shown in equation (14),  $\omega_p = (V/\hbar S) \sqrt{K_{\parallel} K_{\perp}} \epsilon$  is the oscillation frequency in the well for nanometer-scale single-domain ferromagnets at finite magnetic field, and  $S'$  is the total spin of the single-domain FM nanoparticle. From equation (22), the topological quenching of resonant quantum tunneling of the magnetization vector is evident for the half-integer total spin FM nanoparticle in the absence of an external applied magnetic field, resulting from the destructive interference of geometric phase terms in the Euclidean action between topologically different tunneling paths connecting the same initial and final states. Compared with the results in reference [29], both the WKB exponent and the preexponential factors are evaluated exactly in the instanton contribution to the WKB rate for resonant quantum tunneling of the magnetization vector in a single-domain FM nanoparticle placed in an external applied magnetic field along the easy anisotropy axis of the system, opposite to the direction of the magnetization vector. Compared with the AFM case in equations (16), (17), and (18), now the relevant quantity in overlap factors  $\langle \pi/2, \pm\phi_2 | \Psi_r \rangle$  is the total spin for the FM particle. Our theoretical results may be useful in the analysis of further experiments on the observation of the topological phase interference or spin-parity effects in resonant quantum tunneling of the magnetization vector between nonequivalent magnetic wells in nanometer-scale single-domain ferromagnets.

When  $H = 0$  (now  $\phi_2 = \pi$ ), the problem is one of MQC, *i.e.*, the Néel vector resonates coherently between energetically equivalent wells. In discussing MQP, it is essential to distinguish between two types of processes: MQC (*i.e.*, coherent tunneling) and MQT (*i.e.*,

incoherent tunneling). In the case of MQC, the system in question performs coherent NH<sub>3</sub>-type oscillations between two degenerate wells separated by a classically impenetrable barrier. Tunneling between neighboring degenerate vacua can be described by the instanton configuration with nonzero topological charge and leads to a level splitting of the ground states. The tunneling removes the degeneracy of the original ground states, and the true ground state is a superposition of the previous degenerate ground states. For the case of MQT, the system escapes from a metastable potential well into a continuum by quantum tunneling at sufficiently low temperatures, and the tunneling results in an imaginary part of the energy which is dominated by the so-called bounce configuration with zero topological charge [37, 46]. As emphasized by Leggett, the two phenomena of MQC and MQT are physically very different, particularly from the viewpoint of experimental feasibility [31]. MQC is a far more delicate phenomenon than MQT, as it is much more easily destroyed by an environment [47], and by very small  $c$ -number symmetry breaking fields that spoil the degeneracy. The magnetic MQC should show up in resonance measurement of both the magnetic noise and the magnetic susceptibility spectra [19]. Awschalom and co-workers have performed measurements both of the frequency-dependent magnetic susceptibility  $\chi(\omega)$  and the magnetic noise  $S(\omega)$  of ferritin proteins by applying a fully integrated thin-film dc SQUID susceptometer. The key observation is that a well-defined resonance does appear below roughly 200 mK both in  $S(\omega)$  and in the imaginary part,  $\chi''(\omega)$ , of  $\chi(\omega)$ . This resonance can be interpreted as the tunneling level splitting between two macroscopic states of the ferritin particles, namely, the Néel vector pointing up and pointing down. The sharpness of the resonance that Awschalom *et al.* have observed indicates that dissipative coupling to the environment is weak, which is one of the important requirements for observing the phenomenon of MQC. The behavior of the resonance as a function of temperature and the magnetic field is consistent with theoretical expectations for the occurrence of MQC in single-domain anti-ferromagnets, which provides strong support for MQC. In the phenomenon of MQT, the change of magnetization with time is expected to be able to be observed in relaxation-type experiments [48] and compared with theoretical results. The key idea in the magnetic relaxation experiment is to measure the long term magnetization change of a magnetic system after changing the magnetic field applied to it, in which the turning of magnetization vectors is delayed for different time due to the different barriers separating the metastable states. Barbara *et al.* and Tejada *et al.* have made comprehensive studies of the low-temperature magnetic relaxation in different systems (single-domain particles, magnetic grains, layers, multilayers, and random magnets) [48]. The existence of two relaxation regimes has been demonstrated in these systems. At high temperatures, the magnetic viscosity  $S \equiv (1/M_0)(\partial M/\partial \ln(t))$  is proportional to temperature in accordance with theoretical expectation for thermally activated processes. At low temperatures, the viscosity is independent of temperature, providing evidence

to quantum tunneling of magnetization. The key observation is a nonthermal character of the relaxation below a few kelvin, and the transition from the thermal to the nonthermal relaxation regime is sharp. Qualitative agreement between theory and experiment is found, which leads to the consensus on the existence of MQT of magnetization [48].

The classical solution of equation (9) with magnetocrystalline anisotropy equation (4) at zero magnetic field is found to be

$$\begin{aligned}\bar{\theta} &= \pi/2, \\ \sin \bar{\phi} &= \frac{1}{\cosh(\omega_0\tau)}.\end{aligned}\quad (23)$$

Correspondingly, the WKB exponent or the classical action at zero magnetic field is obtained by integrating the Euclidean action (2) with the above classical trajectory,

$$S_{\text{cl}}(H=0) = 2^{3/2} \sqrt{\frac{K_{\parallel}}{J}} S. \quad (24)$$

From equation (20) it is easy to show that if  $S$  is a half-integer, the tunneling rate of single-domain AFM nanoparticles is suppressed to zero no matter whether the excess spin  $s$  is an integer or half-integer. If  $S$  is an integer, the tunneling rate is zero for the half-integer excess spin AFM nanoparticle, but the rate is nonzero for the integer excess spin one. This spin-parity effect is the result of geometric phase interference between topologically distinct tunneling paths. Now the rate of quantum tunneling of the Néel vector in nanometer-scale single-domain antiferromagnets at zero magnetic field is found to be

$$\begin{aligned}\Gamma_{\text{AFM}}(H=0) &= \frac{2^{9/4}}{\pi^{1/2}} \frac{V}{\hbar} K_{\perp} \left( \frac{K_{\parallel} J}{K_{\perp}^2} \right)^{3/4} \\ &\times \exp\left(-4 \frac{K_{\parallel}}{K_{\perp}}\right) S^{-1/2} e^{-S_{\text{cl}}(H=0)},\end{aligned}\quad (25)$$

where the classical action at zero magnetic field is shown in equation (24). The WKB exponent in equation (24) is in good agreement with the result in reference [20]. Therefore, the transition amplitude at zero magnetic field is

$$\begin{aligned}A_{\text{AFM}}(H=0) &= \exp(-\hbar\omega_0 T/2) \\ &\times \exp(i\Gamma_{\text{AFM}}(H=0) T/2) \sum_{m=0}^S (-1)^m C_m,\end{aligned}\quad (26)$$

for  $S$  and  $s$  are both integers.

It has been demonstrated that the tunneling rate is suppressed to zero for a nanometer-scale single-domain antiferromagnet with half-integer excess spin in the absence of the applied magnetic field, due to the destructive phase interference between topological different tunneling paths connecting the same initial and final states. This destructive phase interference or topological quenching effect for the single-domain AFM nanoparticle with

half-integer excess spin is related to a Kramers degeneracy since the system has time-reversal invariance at zero magnetic field. However, in real experiments one will always apply some weak magnetic field which removes the Kramers degeneracy, and then detect the freezing of quantum tunneling in the single-domain AFM nanoparticle with half-integer excess spins. Therefore, the tunneling behaviors of the Néel vector in the presence of a weak applied magnetic field are essential to the experimental observation of the destructive phase interference or topological quenching effect in nanometer-scale single-domain antiferromagnets with half-integer excess spins. However, in a system of a large number of single-domain particles, one would expect statistically equal numbers of integer and half-integer spins. If all moments of the particles are initially magnetized in one direction and then the field is switched off, the freezing effect should reveal itself in a longer magnetic relaxation for the half-integer spin particles. Therefore, the time dependence of the relaxation should show a fast drop of the magnetic moment of the system to one-half of the initial value and then slow relaxation to zero [29]. To observe this effect, one must have a very narrow distribution of particle sizes and magnetic properties, otherwise the broad distribution of individual lifetimes will smear the relaxation. However, unlike most ensembles of magnetic clusters, a macroscopic sample of molecular magnets (such as  $\text{Mn}_{12}\text{ac}$  [41], or  $\text{Fe}_8$  [42,43]) consists of a large (Avogadro's) number of identical particles with the same magnetic properties and identical characteristic energies, allowing much more accurate comparisons with theory to be made. Now we consider the limiting case that  $H/H_c \rightarrow 0$ . The classical solution of equation (9) with the magnetocrystalline anisotropy equation (4) in the weak field limit is found to be

$$\begin{aligned}\bar{\theta} &= \pi/2, \\ \sin \bar{\phi} &= \frac{1}{\cosh(\omega_1\tau)},\end{aligned}\quad (27)$$

where  $\omega_1 = (V/\hbar S) \sqrt{2K_{\parallel}J} (1 - H/2H_c)$ . The corresponding classical action can be evaluated by integrating the Euclidean action (2) with the above classical trajectories, and the result is

$$S_{\text{cl}}(H/H_c \rightarrow 0) = 2^{3/2} \sqrt{\frac{K_{\parallel}}{J}} \left[ 1 - \frac{1}{2} \left( \frac{H}{H_c} \right) \right] S. \quad (28)$$

For the present case,  $\phi_2$  is very close to  $\pi$ . Introducing  $\phi_2 = \pi - \delta$ , where  $\delta = 2\sqrt{H/H_c}$ , we obtain the WKB rates for resonant quantum tunneling of the Néel vector between nonequivalent magnetic wells for the weak field limit by applying the formulas in reference [24],

$$\begin{aligned}\Gamma_{\text{AFM}} &= \frac{2^{9/4}}{\pi^{1/2}} \frac{V}{\hbar} K_{\perp} \left( \frac{K_{\parallel} J}{K_{\perp}^2} \right)^{3/4} \left[ 1 - \left( \frac{5}{4} - \frac{1}{2} \frac{K_{\parallel}}{K_{\perp}} \right) \left( \frac{H}{H_c} \right) \right] \\ &\times \exp\left\{-4 \left( \frac{K_{\parallel}}{K_{\perp}} \right) \times \left[ 1 - \left( 1 - \frac{K_{\parallel}}{K_{\perp}} \right) \left( \frac{H}{H_c} \right) \right]\right\} \\ &\times S^{-1/2} e^{-S_{\text{cl}}(H/H_c \rightarrow 0)},\end{aligned}\quad (29)$$



where the classical action in the weak field limit is shown in equation (27). Therefore, the transition amplitude at weak field limit is found to be

$$A_{\text{AFM}} = \exp(-\hbar\omega_1 T/2) \exp(i\Gamma_{\text{AFM}} T/2) \times \begin{cases} \cos[(S-s)\delta] \sum_{m=0}^S C_m \cos(m\delta), \\ \quad S, s = \text{integer}, \\ \sin[(S-s)\delta] \sum_{m=0}^S C_m \cos(m\delta), \\ \quad S = \text{integer}, s = \text{half-integer}, \\ \sin[(S-s)\delta] \sum_{m=0}^{S-1/2} C_m \sin[(m+1/2)\delta], \\ \quad S = \text{half-integer}, s = \text{integer}, \\ \cos[(S-s)\delta] \sum_{m=0}^{S-1/2} C_m \sin[(m+1/2)\delta], \\ \quad S, s = \text{half-integer}, \end{cases} \quad (30)$$

To summarize, we have investigated the topological phase interference or spin-parity effects in resonant quantum tunneling of the Néel vector in nanometer-scale single-domain antiferromagnets between nonequivalent wells formed by the external magnetic field applied along the easy anisotropy axis of the system, opposite to the direction of the Néel vector, based on the two-sublattice model. Both the WKB exponent and the preexponential factors in the instanton's contribution to the rate of quantum tunneling of the Néel vector are obtained exactly for the entire region of the external magnetic field ( $0 \leq H < H_c$ ) by applying the standard instanton technique in the spin-coherent-state path-integral representation, which should be useful for a quantitative understanding of further experiments on the topological phase interference effects in resonant quantum tunneling of the Néel vector between nonequivalent magnetic wells in single-domain AFM nanoparticles. The WKB exponent at zero magnetic field is consistent with the result in reference [20], and the suppression of resonant quantum tunneling of the Néel vector by destructive interfering topological phase terms in the Euclidean action is evident for the single-domain AFM nanoparticle with half-integer excess spins. Another important observation is that the WKB rates of quantum tunneling of the Néel vector for both integer and half-integer excess spins oscillate with the external magnetic field applied along the easy anisotropy axis of the system. And the oscillation of WKB rate with the applied field for half-integer excess spins is found to be significantly different from that for integer excess spins, resulting from the geometric phase interference between topologically distinct tunneling paths connecting the same initial and final states. Note that these quantum phase interference effects are of topological origin, and therefore are independent of the magnitude of the excess spin of the single-domain AFM nanoparticle. The tunneling behaviors in resonant quantum transition of the magnetization vector between nonequivalent magnetic wells are also obtained for the nanometer-scale single-domain ferromagnets with biaxial crystal symmetry in the presence of the external magnetic field applied along the easy anisotropy

axis by making use of the similar technique as that for the nanometer-scale single-domain antiferromagnets, but in the large noncompensation limit.

At the end of this paper, we discuss the experimental condition of the external applied magnetic field for observing the destructive phase interference or topological quenching effect in single-domain AFM nanoparticles with half-integer excess spins. For AFM nanoparticles with half-integer excess spins in the absence of an external applied magnetic field, it has been theoretically demonstrated that there is no resonant quantum tunneling taking place between two energy minima of the system, resulting from the destructive interference of the Berry phase or the Wess-Zumino, Chern-Simons term in the Euclidean action between the topologically different tunneling paths of the clockwise ( $\Delta\phi = -\pi$ ) and the counter-clockwise ( $\Delta\phi = \pi$ ) instantons. Such destructive phase interference or topological quenching effect for half-integer excess spins is related to the Kramers' degeneracy due to the time-reversal invariance of the system in the absence of an external applied magnetic field. Therefore, the ground state is a Kramers doublet so long as the excess spin of the single-domain AFM nanoparticle is a half-integer, which, according to the Kramers' theorem, leads to the absence of resonant quantum tunneling of the Néel vector between energetically degenerate easy directions. However, in real experiments, in order to detect the freezing of resonant quantum tunneling of the Néel vector for the single-domain AFM nanoparticle with half-integer excess spins, one will always apply a weak magnetic field to remove the Kramers' degeneracy. This field satisfies the condition that the Zeeman energy splitting must be much smaller than the energy level difference,  $\Delta E = \hbar\omega_0$ , in one of the magnetic wells at zero field, which means that

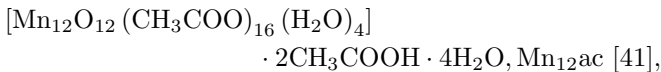
$$H \ll \frac{V}{\hbar\gamma} \frac{1}{Ss} \sqrt{2K_{\parallel} J}. \quad (31)$$

*i.e.*, the traces of topological quenching effect will be destroyed when the field is large enough to make the ground state in one well degenerate with the first excited state in the other well.

Typical values of the parameters for the exchange energy density between two sublattices and the longitudinal anisotropy coefficient for the single-domain AFM nanoparticle are  $J \sim 10^{10}$  erg/cm<sup>3</sup> and  $K_{\parallel} \sim 10^5$  erg/cm<sup>3</sup>. The radius of the single-domain AFM nanoparticle is about 5 nm. The number of spins in one sublattice is about  $10^3$  and the number of excess spins in the single-domain AFM nanoparticle due to the small noncompensation of two sublattices is about 10. Substituting these values into equation (27), we suggest that  $H \sim 100$  Oe to observe the destructive phase interference or topological quenching effect for single-domain AFM nanoparticles with half-integer excess spins in experiments. This condition will be easier to be satisfied in the single-domain AFM nanoparticle than in the single-domain FM nanoparticle of a comparable size [34]. It is noted that all calculations performed in this paper are based on the two-sublattice model for single-domain AFM particles. We find that

$H_c \approx 1.13 \times 10^6$  Oe, and  $H_{s.f.} = 1.53 \times 10^6$  Oe for typical values of parameters for nanometer-scale single-domain antiferromagnets. Therefore, the coercive field is smaller than the spin-flop field, at which the two-sublattice configuration is valid for single-domain AFM nanoparticles at finite magnetic field.

Recent experiments have rekindled interest in the field of quantum tunneling of magnetization. Most notable has been the discovery of resonant quantum tunneling between spin states in the systems of spin-10 molecules such as a dodecanuclear mixed-valence manganese-oxo cluster with acetate ligands of formula



and an octanuclear iron(III) oxo-hydroxo cluster of formula  $[\text{Fe}_8\text{O}_2(\text{OH})_{12}(\text{tacn})_6]^{8+}$ ,  $\text{Fe}_8$  [42,43], where tacn is the organic ligand triazacyclononane. At low temperatures the magnetization in these systems are found to relax significantly faster at particular values of magnetic field that correspond to resonance between spin states. More recently, Wernsdorfer and Sessoli have measured the tunneling splittings on the order of  $10^{-8}$  K in the molecular  $\text{Fe}_8$  clusters with the help of an array of micro-SQUIDS with a very high sensitivity [40]. They have found a very clear oscillation in the tunneling splittings, which is direct evidence of the role of the topological spin phase (Berry phase) in the spin dynamics of these molecules. It is noted that the theoretical results presented in this paper are based on the standard instanton technique in the spin-coherent-state path-integral representation, which is semiclassical in nature, *i.e.*, valid for large spins and in the continuum limit. Whether the instanton technique can be applied in studying the spin dynamics in magnetic molecular clusters with  $S = 10$  (such as  $\text{Fe}_8$ ) is an open question. Work is now in progress to investigate the spin-parity or topological phase interference effects in resonant quantum tunneling of magnetization in magnetic molecular clusters.

Various dissipative effects caused by the interactions with the environment such as phonons [44], nuclear spins [45], and Stoner excitations and eddy currents in metallic magnets [15] are important in macroscopic quantum tunneling of magnetism. The most important is, however, the interaction between spins of the magnets and spins of the environment, since the change of a single  $1/2$  spin would transform the constructive interference to destructive or *vice versa*. Loss *et al.* [49] discussed the spin-parity effect in the presence of dissipation by applying three different techniques, due to Feynman and Vernon [50–52], Caldeira and Leggett [2], and Franck and Condon [53]. They found that the Feynman-Vernon calculation indicates that the spin-parity effect is reduced by dissipation, that is, coupling to the environment does produce tunneling for half-integer spins. On the other hand, the Caldeira-Leggett and Franck-Condon computations predict the absence of any tunnel splitting of the ground-state for half-integer spins, *i.e.*, the spin-parity can be said to survive coupling to the environment. So the actual situation is more complicated and work along this line is still

in progress. We hope that the theoretical results obtained in the present work will stimulate more experiments whose aim is observing the topological phase interference or spin-parity effects in resonant quantum tunneling of the Néel vector in nanometer-scale single-domain antiferromagnets.

One of the authors (R.L.) is very thankful to Dr. Jian Wu, Dr. Jian-She Liu, and Professor Zhan Xu for many useful discussions. R.L. also thanks Institute of Theoretical Physics, Shanxi University for its hospitality during his visit here, and Yun-Bo Zhang, Yi-Hang Nie, Shu-Peng Kou, Professor Jiu-Qing Liang and Professor Fu-Cho Pu for enlightening discussions and providing their papers before publication. R.L. and J.-L. Zhu would like to thank Professor W. Wernsdorfer and Professor R. Sessoli for providing their paper (Ref. [40]).

## Appendix A: Evaluation of the preexponential factors in WKB tunneling rate

In this appendix, we review briefly the procedure on how to calculate the preexponential factors in the WKB rate of quantum tunneling of the Néel vector in single-domain AFM nanoparticles, based on the two-sublattice model and the standard instanton technique in the spin-coherent-state path-integral representation [11,24,35–37]. The preexponential factors in WKB tunneling rate are due to the quantum fluctuations about the classical path, which can be evaluated by expanding the Euclidean action to second order in small fluctuations. Then we apply this approach to obtain the instanton's contribution to the tunneling rates for resonant quantum transition of the Néel vector between nonequivalent magnetic wells in single-domain AFM nanoparticles with biaxial crystal symmetry in the presence of an external magnetic field applied along the easy anisotropy axis.

In reference [24], Lü *et al.* have studied the general formulas for evaluating both the WKB exponent and the preexponential factors in the tunneling rate (MQT) or the tunneling level splitting (MQC) for the single-domain AFM nanoparticles based on the two-sublattice model and the standard instanton technique in the spin-coherent-state path-integral representation, without assuming a specific form of the magnetocrystalline anisotropy and the external applied magnetic field. Here we explain briefly the basic idea of this calculation. Such a calculation consists of two major steps. The first step is to find the classical, or least-action path (instanton) from the classical equations of motion for the Néel vector in single-domain AFM nanoparticles, which gives the exponent or the classical action in the WKB tunneling rate. Instantons in one-dimensional field theory can be viewed as pseudoparticles with trajectories existing in the energy barrier, and are therefore responsible for quantum tunneling. The second step is to expand the Euclidean action to second order in the small fluctuations about the classical path, and then evaluate the Van Vleck determinant of resulting quadratic form [24,35–37]. For single-domain AFM nanoparticles, writing  $\theta(\tau) = \bar{\theta}(\tau) + \theta_1(\tau)$  and

$\phi(\tau) = \bar{\phi}(\tau) + \phi_1(\tau)$ , where  $\bar{\theta}$  and  $\bar{\phi}$  denote the classical path, one obtains the Euclidean action of equation (2) as  $S_E[\theta(\tau), \phi(\tau)] \approx S_{cl} + \delta^2 S$  with  $S_{cl}$  being the classical action or the WKB exponent and  $\delta^2 S$  being a functional of small fluctuations  $\theta_1$  and  $\phi_1$  [24],

$$\delta^2 S = \frac{V}{\hbar} \int d\tau \left[ \frac{\chi_{\perp}}{2\gamma^2} \left( \frac{d\theta_1}{d\tau} \right)^2 + \frac{\chi_{\perp}}{2\gamma^2} \sin^2 \bar{\theta} \left( \frac{d\phi_1}{d\tau} \right)^2 + \frac{\chi_{\perp}}{\gamma^2} \sin(2\bar{\theta}) \left( \frac{d\bar{\phi}}{d\tau} \right) \left( \frac{d\phi_1}{d\tau} \right) \theta_1 + \frac{\chi_{\perp}}{2\gamma^2} \cos(2\bar{\theta}) \left( \frac{d\bar{\phi}}{d\tau} \right)^2 \theta_1^2 + \frac{1}{2} (E_{\theta\theta}\theta_1^2 + 2E_{\theta\phi}\theta_1\phi_1 + E_{\phi\phi}\phi_1^2) \right], \quad (\text{A.1})$$

where

$$E_{\theta\theta} = (\partial^2 E / \partial \theta^2)_{\theta=\bar{\theta}, \phi=\bar{\phi}}, E_{\theta\phi} = (\partial^2 E / \partial \theta \partial \phi)_{\theta=\bar{\theta}, \phi=\bar{\phi}},$$

and  $E_{\phi\phi} = (\partial^2 E / \partial \phi^2)_{\theta=\bar{\theta}, \phi=\bar{\phi}}$ .

Under the condition that

$$(1/2) E_{\theta\theta} + (\chi_{\perp}/2\gamma^2) (\cos 2\bar{\theta}) (d\bar{\phi}/d\tau)^2 > 0,$$

where  $E_{\theta\theta}$  is evaluated at the classical path, the Gaussian integration can be performed over  $\theta_1$ , and the remaining  $\phi_1$  path integral can be casted into the standard form for a one-dimensional motion problem. As usual there exists a zero-mode,  $d\bar{\phi}/d\tau$ , corresponding to a translation of the center of the instanton, and a negative eigenvalue in the MQT problem [24, 35–37]. This leads to the imaginary part of the energy, which corresponds to the quantum escaping rate from the metastable state through the classically impenetrable barrier to a stable one. The resonant tunneling splittings of the ground state for the MQC problem of the Néel vector can be evaluated by applying the similar technique [11, 24, 35–37]. What is need for the calculation of the tunneling rate (in MQT) and the tunneling level splitting (in MQC) is the asymptotic relation of the zero mode,  $d\bar{\phi}/d\tau$ , for large  $\tau$  [11, 24, 35–37],

$$d\bar{\phi}/d\tau \approx ae^{-\mu\zeta}, \quad \text{as } \zeta \rightarrow \infty. \quad (\text{A.2})$$

The new time variable  $\zeta$  in equation (A.2) is related to  $\tau$  as

$$d\zeta = d\tau/2A(\bar{\theta}(\tau), \bar{\phi}(\tau)), \quad (\text{A.3})$$

where

$$A(\bar{\theta}, \bar{\phi}) = J \frac{V}{\hbar} \frac{\chi_{\perp}}{2\gamma^2} \frac{\sin^2 \bar{\theta}}{E_{\phi\phi}(\bar{\theta}, \bar{\phi}) + (\chi_{\perp}/\gamma^2) (\cos 2\bar{\theta}) (d\bar{\phi}/d\tau)^2}. \quad (\text{A.4})$$

Then the instanton's contribution to the tunneling rate for MQT or the tunneling level splitting for MQC of the Néel vector in single-domain AFM nanoparticles (without the contribution of the topological phase term in the Euclidean action) is given by [11, 24, 35–37]

$$|a| (\mu/\pi)^{1/2} e^{-S_{cl}}. \quad (\text{A.5})$$

Therefore, all that is necessary is to differentiate the classical path (instanton) to obtain  $d\bar{\phi}/d\tau$ , then convert from  $\tau$  to the new time variable  $\zeta$  according to equations (A.3, A.4), and read off  $a$  and  $\mu$  by comparison with equation (A.2). If the condition  $(1/2) E_{\phi\phi} + (\chi_{\perp}/2\gamma^2) (\cos 2\bar{\theta}) (d\bar{\phi}/d\tau)^2 > 0$  is not satisfied, one can always perform the Gaussian integration over  $\phi_1$  and end up with a one-dimensional path integral over  $\theta_1$  [24].

Now we apply this approach to the single-domain AFM nanoparticle with biaxial crystal symmetry in the presence of an external magnetic field applied along the easy anisotropy axis, opposite to the direction of the Néel vector. After some algebra, we find that

$$\frac{1}{2} E_{\theta\theta} + \frac{\chi_{\perp}}{2\gamma^2} \cos 2\bar{\theta} \left( \frac{d\bar{\phi}}{d\tau} \right)^2 = K_{\perp} - 2K_{\parallel} \sin^2 \phi - 2K_{\parallel} \left( \frac{H}{H_c} \right) \left( 1 - \frac{1}{2} \cos \phi \right) = K_{\perp} + O(K_{\parallel}), \quad (\text{A.6})$$

which is positive. So we can perform the Gaussian integration over  $\theta_1$  directly. And after some complicated calculations, we obtain the following relation between  $\tau$  and the new imaginary-time variable  $\zeta$  for this MQT problem,

$$\tau = \frac{\hbar S^2}{2K_{\perp} V} \frac{1}{1 - \left( \frac{K_{\parallel}}{K_{\perp}} \right) \left( \frac{H}{H_c} \right)} \zeta + \left( \frac{K_{\parallel}}{K_{\perp}} \right) \frac{1}{1 - \left( \frac{K_{\parallel}}{K_{\perp}} \right) \left( \frac{H}{H_c} \right)} \times \frac{1}{\omega_0} \left[ 4\sqrt{\epsilon} + 3(1 - \epsilon) \ln \left( \frac{1 + \sqrt{\epsilon}}{1 - \sqrt{\epsilon}} \right) \right]. \quad (\text{A.7})$$

It is easy to differentiate the instanton solution to obtain

$$\frac{d\bar{\phi}}{d\tau} = 4 \frac{V}{\hbar S} \sqrt{2K_{\parallel} J} \frac{\epsilon}{\sqrt{1 - \epsilon}} \left( \frac{1 + \sqrt{\epsilon}}{1 - \sqrt{\epsilon}} \right)^{3 \frac{\left( \frac{K_{\parallel}}{K_{\perp}} \right) \left( \frac{H}{H_c} \right)}{1 - \left( \frac{K_{\parallel}}{K_{\perp}} \right) \left( \frac{H}{H_c} \right)} \sqrt{\epsilon}} \times \exp \left[ -4 \left( \frac{K_{\parallel}}{K_{\perp}} \right) \frac{1}{1 - \left( \frac{K_{\parallel}}{K_{\perp}} \right) \left( \frac{H}{H_c} \right)} \epsilon \right] \times \exp \left[ -\sqrt{\frac{K_{\parallel} J \epsilon}{2K_{\perp}^2}} \frac{1}{1 - \left( \frac{K_{\parallel}}{K_{\perp}} \right) \left( \frac{H}{H_c} \right)} S \zeta \right] \quad \text{as } \zeta \rightarrow \infty. \quad (\text{A.8})$$

Thus, reading off  $|a|$  and  $\mu$  in equation (A.8), we obtain the instanton's contribution to the WKB tunneling rate shown in equations (12, 13) for resonant quantum transition of the Néel vector between nonequivalent wells formed by the external magnetic field applied along the easy anisotropy axis of the system, opposite to the direction of the Néel vector.

## References

1. A.O. Caldeira, A.J. Leggett, Phys. Rev. Lett. **46**, 211 (1981).
2. A.O. Caldeira, A.J. Leggett, Ann. Phys. **149**, 374 (1983).
3. S. Chakravarty, A.J. Leggett, Phys. Rev. Lett. **52**, 5 (1984).
4. A.J. Leggett, S. Chakravarty, A.T. Dorsey, M.P.A. Fisher, A. Garg, W. Zwerger, Rev. Mod. Phys. **59**, 1 (1987).
5. R.F. Voss, R.A. Webb, Phys. Rev. Lett. **49**, 697 (1981); S. Washburn, R.A. Webb, R.F. Voss, S.M. Faris, Phys. Rev. Lett. **54**, 2712 (1985); J.M. Martinis, M.H. Devoret, J. Clarke, Phys. Rev. Lett. **55**, 1543 (1985); M.H. Devoret, J.M. Martinis, J. Clarke, Phys. Rev. B **37**, 5950 (1988).
6. U. Eckern, G. Schön, V. Ambegaokar, Phys. Rev. B **30**, 6419(1984); H. Simanjuntak, L. Gunther, J. Low Temp. Phys. **78**, 131 (1990).
7. H. Simanjuntak, L. Gunther, Phys. Rev. B **42**, 930 (1991).
8. W. den Boer, R. de Bruyn Ouboter, Physica B **98**, 185 (1980); R.J. Prance, A.P. Long, T.D. Clark, A. Widom, J.E. Mutton, J.Sacco, M.W. Potts, G. Megaloudis, F. Goodall, Nature **289**, 543 (1980); D.W. Bol, J.J.F. Scheffer, W.T. Giele, R. Ouboter de Bruyn, Physica B **133**, 196 (1985); D.B. Schwartz, B. Sen, C.N. Archie, J.E. Lukens, Phys. Rev. Lett. **55**, 1547 (1985).
9. E.M. Chudnovsky, L. Gunther, Phys. Rev. Lett. **60**, 661 (1988).
10. A. Garg, G.H. Kim, J. Appl. Phys. **67**, 5669 (1990).
11. A. Garg, G.H. Kim, Phys. Rev. B **45**, 12921 (1992).
12. E.M. Chudnovsky, L. Gunther, Phys. Rev. B **37**, 9455 (1988).
13. P.C.E. Stamp, Phys. Rev. Lett. **66**, 2802 (1991).
14. E.M. Chudnovsky, O. Iglesias, P.C.E. Stamp, Phys. Rev. B **46**, 5392 (1992).
15. G. Tataru, H. Fukuyama, Phys. Rev. Lett. **72**, 772 (1994).
16. D.D. Awschalom, M.A. McCord, G. Grinstein, Phys. Rev. Lett. **65**, 783 (1990).
17. C. Paulsen, L.C. Sampaio, B. Barbara, D. Fruchart, A. Marchand, J.L. Tholence, M. Uehara, Phys. Lett. A **161**, 319 (1991).
18. X.X. Zhang, L.I. Balcells, J. M. Ruiz, J.L. Tholence, B. Barbara, J. Tejada, J. Phys. Cond. Matter **4** L163 (1992); X.X. Zhang, L.I. Balcells, J.M. Ruiz, O. Iglesias, J. Tejada, B. Barbara, Phys. Lett. A **163**, 130 (1992).
19. D.D. Awschalom, J.F. Smyth, G. Grinstein, D.P. DiVincenzo, D. Loss, Phys. Rev. Lett. **68**, 3092 (1992).
20. B. Barbara, E.M. Chudnovsky, Phys. Lett. A **145**, 205 (1990); E.M. Chudnovsky, J. Magn. Magn. Mater. **140-144**, 1821 (1995).
21. J.M. Duan, A. Garg, J. Phys. Cond. Matter **7**, 2171 (1995).
22. I.V. Krive, O.B. Zaslavskii, J. Phys. Cond. Matter **2**, 9457 (1990).
23. H. Simanjuntak, J. Phys. Cond. Matter **6**, 2925 (1994).
24. Rong Lü, Jia-Lin Zhu, Xi Chen, Lee Chang, J. Phys. Cond. Matter **10**, 3595 (1998).
25. D. Loss, D.P. DiVincenzo, G. Grinstein, Phys. Rev. Lett. **69**, 3232 (1992).
26. J.V. Delft, G. L. Henley, Phys. Rev. Lett. **69**, 3236 (1992).
27. A. Garg, Europhys. Lett. **22**, 205 (1993).
28. Rong Lü, Jia-Lin Zhu, Xi Chen, Lee Chang, Eur. Phys. J. B **3**, 35 (1998). In reference [28], we have investigated the resonant quantum tunneling of the Néel vector in a single-domain AFM nanoparticle in the presence of an external magnetic field applied along the hard anisotropy axis of the system (compared with the easy anisotropy axis in the present work). The magnetocrystalline anisotropy and the external applied magnetic field create equivalent wells (compared with the nonequivalent wells in the present work) along the  $\phi$  coordinate. Our results show that the tunneling behavior of the Néel vector between nonequivalent wells is significantly different from that of the Néel vector between equivalent wells. Therefore, the theoretical results obtained in the present work may be useful in the analysis of further experiments on the observation of the spin-parity or topological phase interference effects in resonant quantum tunneling of the Néel vector between nonequivalent magnetic wells in single-domain AFM nanoparticles with biaxial crystal symmetry in the presence of an external magnetic field applied along the easy anisotropy axis of the system.
29. E.M. Chudnovsky, D.P. DiVincenzo, Phys. Rev. B **48**, 10548 (1993).
30. A. Garg, Phys. Rev. B **51**, 15161 (1995).
31. A.J. Leggett, in Essays in *Theoretical Physics in Honour of Dirk ter Haar* (Pergamon, Oxford, 1984); *Quantum Tunneling of Magnetization*, edited by L. Gunther, B. Barbara (Kluwer, Dordrecht, the Netherlands, 1995).
32. D.P. DiVincenzo, Phys. Rev. A **51**, 1015 (1995); D. Loss, D.P. DiVincenzo, *ibid.* **57**, 120 (1998); D.P. DiVincenzo, P.W. Shor, J.A. Smolin, *ibid.* **57**, 830 (1998), and references therein.
33. S. Lloyd, Science **261**, 1569 (1993); *ibid.* **263**, 695 (1994); D.P. DiVincenzo, *ibid.* **269**, 255 (1995).
34. For the nanometer-scale single-domain ferromagnets with biaxial crystal symmetry, the experimental condition of the external applied magnetic field for observing the destructive phase interference or topological quenching effect for the half-integer total spins can be obtained by making use of the similar technique as that for nanometer-scale single-domain antiferromagnets, and the result is found to be  $H \ll (H_c/S')\sqrt{K_\perp/K_\parallel}$ , where  $S'$  is the total spin of the single-domain FM nanoparticle.  $H_c = 2K_\parallel/M_0$  is the coercive field for the single-domain FM nanoparticle at which the initial state becomes classically unstable, where  $M_0 = \hbar\gamma S'/V$  is the magnitude of total magnetization moment in the FM particle. Compared with the results in reference [29], our condition has an additional prefactor which is related to the ratio of the transverse anisotropy coefficient to the longitudinal one. It has been pointed out that the rate of quantum tunneling of the magnetization vector is small unless the ratio of the transverse anisotropy coefficient to the longitudinal one is large for nanometer-scale single-domain ferromagnets in the absence of an external applied magnetic field. Therefore, for the highly anisotropic materials (such as the rare-earth materials) in experiments, this prefactor in our condition for the external applied magnetic field will be important. Taking the typical values of parameters for the single-domain FM nanoparticle, we find that the external applied magnetic field will be of the order of 10 Oe, which is smaller than that for the single-domain AFM nanoparticle of a comparable size.
35. S. Coleman, Phys. Rev. D **15**, 2929 (1977).
36. C.G. Callan, S. Coleman, Phys. Rev. D **16**, 1762 (1977).

37. S. Coleman, *Aspects of Symmetry* (Cambridge University Press, Cambridge, England, 1985), Chap. 7.
38. F.D.M. Haldane, Phys. Rev. Lett. **50**, 1153 (1983).
39. I. Affleck, J. Phys. Cond. Matter **1**, 3047 (1989).
40. W. Wernsdorfer, R. Sessoli, Science **284**, 133 (1999).
41. R. Sessoli, D. Gatteschi, A. Caneschi, M.A. Novak, Nature **365**, 141 (1993).
42. A.-L. Barra, P. Debrunner, D. Gatteschi, C.E. Schulz, R. Sessoli, Europhys. Lett. **35**, 133 (1996).
43. C. Sangregorio, T. Ohm, C. Paulsen, R. Sessoli, D. Gatteschi, Phys. Rev. Lett. **78**, 4645 (1997).
44. A. Garg, G.-H. Kim, Phys. Rev. Lett. **63**, 2512 (1989); Phys. Rev. B **43**, 712 (1991).
45. A. Garg, J. Appl. Phys. **76**, 6168 (1994).
46. J.-Q. Liang, H.J.W. Müller-Kirstein, Jian-Ge Zhou, Z. Phys. B **102**, 525 (1997).
47. A. Garg, J. Appl. Phys. **76**, 6168 (1994); Phys. Rev. Lett. **74**, 1458 (1995).
48. B. Barbara, L.C. Sampaio, J.E. Wegrowe, B.A. Ratnam, A. Marchand, C. Paulsen, M.A. Novak, J.L. Tholence, M. Uehara, D. Fruchart, J. Appl. Phys. **73**, 6703 (1993) and references therein; J. Tejada, X.X. Zhang, J. Appl. Phys. **73**, 6709 (1993) and reference therein.
49. D. Loss, D.P. DiVincenzo, G. Grinstein, D.D. Awschalom, J.F. Smyth, Physica B **189**, 189 (1993).
50. R.P. Feynman, F.L. Vernon, Ann. Phys. **24**, 118 (1963).
51. R.P. Feynman, A.R. Hibbs, *Quantum mechanics and Path integrals* (McGraw-Hill, New York, 1965).
52. A.O. Caldeira, A.J. Leggett, Physica A **121**, 587 (1983).
53. See: *e.g.*, J.P. Sethna, Phys. Rev. B **24**, 698 (1981), and references therein.